Few-shot Fine-grained Classification of Histological Images

Yingdong Jiang
College of Software
Jilin University
Key Laboratory of Symbolic Computation and Knowledge Engineering of Ministry of Education
Jilin University
ChangChun, China
ydjiang21@mails.jlu.edu.cn

Jing Huang*
College of Computer Science and Technology
Jilin University
Key Laboratory of Symbolic Computation and Knowledge Engineering of Ministry of Education
Jilin University
ChangChun, China
huangjing@jlu.edu.cn

Zihe Jin
College of Computer Science and Technology
Jilin University
ChangChun, China
jinzh2121@mails.jlu.edu.cn

Leqi Shen
College of Computer Science and Technology
Jilin University
ChangChun, China
shenlq2121@mails.jlu.edu.cn

Ziyi Zhang
College of Computer Science and Technology
Jilin University
ChangChun, China
zhangzy2121@mails.jlu.edu.cn

2023 IEEE International Conference on Medical Artificial Intelligence (MedAI) | 979-8-3503-5878-0/23/$31.00 ©2023 IEEE | DOI: 10.1109/MEDAI59581.2023.00056

***Abstract*—Histological image classification plays a crucial role in cancer diagnosis. However, the acquisition of well-labeled histological images is prohibitively expensive, and obtaining rare abnormal samples is challenging. Therefore, applying few-shot learning methods to histological image classification tasks holds significant clinical value. Nevertheless, existing research predominantly relies on coarse-grained image classification approaches based on natural image datasets, which struggle to address the fine-grained challenges encountered in histological image classification, such as intra-class diversity and inter-class similarity. To tackle this issue, this study proposes a novel few-shot fine-grained classification method for histological images, named "Category-Aware Feature Map Reconstruction Network." This method employs channel weights to localize the differences between inter-class and intra-class regions, composed of intra-class channel weights and inter-class channel weights, collectively referred to as category-aware weights. Specifically, intra-class channel weights indicate the matching degree of salient regions within the support set of a particular class, while inter-class channel weights represent the degree of containing distinct information between classes. The category-aware weights are utilized to transform the support feature maps and query feature maps, generating feature maps that capture differentiating details between categories. Finally, the distance between the transformed query feature map and support feature map is calculated to achieve probabilistic predictions for the categories. On a histological few-shot dataset, this method achieves an accuracy of 90.23% using ResNet-12 as the feature extractor, surpassing the baseline model by 5.24% and outperforming other few-shot methods by at least 10% in the 5-way 10-shot experimental setting. The proposed method exhibits exceptional performance on histological image few-shot datasets, playing a vital role in more accurate and pathologist-independent cancer diagnosis.**

***Index Terms*—Computer-aided diagnosis ,Few-shot learning, Fine-grained classification ,Histological image classification ,Convolutional neural networks ,Attention mechanism**

I. Introduction

Cancer is one of the significant diseases that result in many deaths worldwide, and its incidence continues to increase annually. With hundreds of different types, cancer classification has become increasingly complex and challenging[1][2]. Histological images provide important phenotypic and diagnostic information for evaluating and predicting diseases, thus critical in cancer diagnosis and treatment [3]. However, the current approach relies mainly on pathologists for manual diagnosis, which is time-consuming, laborious, and dependent on the pathologist's experience. Therefore, developing automated histological image classification methods is paramount for cancer diagnosis.

Deep learning has made significant progress in image classification tasks in recent years, but it relies heavily on labeled data. When labeled data is scarce, the generalization ability of deep learning models is poor, which limits their development. To address this problem, few-shot learning has emerged as a solution, allowing deep learning models to classify new image classes using only a few samples. Although many new methods and research have been proposed, they have been applied to natural images, significantly different from histological images. Background information and target regions belong to the same tissue area without clear boundaries in histological images. Moreover, a single histological image usually contains multiple scattered targets that must be identified. These factors pose the challenge of intra-class diversity and inter-class similarity. Thus greater emphasis must be placed on the fine-grained attributes of the images in few-shot classification tasks of histological images.

979-8-3503-5878-0/23/$31.00 ©2023 IEEE
DOI 10.1109/MedAI59581.2023.00056

Authorized licensed use limited to: JILIN UNIVERSITY. Downloaded on April 02,2024 at 06:48:38 UTC from IEEE Xplore. Restrictions apply.

Few-shot learning can be divided into optimization-based methods [4] and metric-based methods [5][6][7][8]. Optimization-based methods originated from the MAML algorithm [4], which aims to enable the model to learn suitable initialization parameters, thereby improving its overall performance on new tasks. Although Chao et al. [9] achieved better metric performance than traditional methods in few-shot classification tasks for histological images using the MAML method, its clinical application still requires further exploration. This may be because optimization-based methods focus more on overall performance while losing the ability to capture fine-grained information for specific tasks. In contrast, metric-based methods focus on learning deep representation to classify images of new classes. Compared to optimization-based methods, metric-based methods can capture more fine-grained information.

Metric-based methods can be divided into global feature methods[5] and local feature methods[7][8][10]. Global feature methods use the global average pooling of the feature map extracted by the convolutional feature extractor as the feature representation. Still, they may lose the spatial details essential for fine-grained classification. In contrast, local feature-based methods use a set of deep descriptors of the feature map as the feature representation that contains the spatial details of the image and constitutes the essential input for fine-grained classification. Therefore, the local feature-based method is suitable for solving the classification problem of few-shot fine-grained histological images.

Feature Map Reconstruction Network (FRN) [8] is a state-of-the-art local feature-based method that resolves spatial mismatches between critical features on different feature maps through spatial alignment techniques. However, the performance of the method is limited on fine-grained image tasks, probably because its features for de-scribing new objects are not discriminative enough in the corresponding tasks[11]. Therefore, this study proposes a category-aware feature map reconstruction network method. The method uses category-aware weights to weigh the channels of the feature maps of each class to identify the representative channels of each class and locate the different regions. Then, the category-aware weights are used to transform the support and query feature maps to obtain the feature maps that can highlight the specific details between classes. Finally, the prediction of class probabilities is accomplished by calculating the distance between the transformed feature maps.

The main contributions of this study are twofold.

(1) We propose a category-aware Feature Map Reconstruction Network method for the few-shot fine-grained classification of histological images. This method is the first to explore the task of a few-shot fine-grained classification of histological images.

(2) We establish a public few-shot histological image dataset and validate our proposed method's performance on this dataset. The experimental results show that under the 5-way 10-shot experimental setting, our method achieves an accuracy of 90.23%, a 5.24% improvement over the baseline model.

II. Methodology

This section presents the overall architecture of the proposed Category-Aware Feature Map Reconstruction Network.

A. Architecture Overview

The architecture of our proposed Category-Aware Feature Map Reconstruction Network is illustrated in Figure 1. Firstly, a convolutional feature extractor is utilized to extract features from both the support and query images, resulting in support feature maps and query feature maps. Subsequently, category-aware weights are computed based on the support feature maps. These weights enhance the discriminability of channels, enabling focused attention on differentiating details between intra-class and inter-class feature maps. Lastly, the support feature maps and query feature maps are transformed into feature maps that specifically capture inter-class discriminative details using the category-aware weights. The final distance calculation is performed on the transformed feature maps to achieve probabilistic predictions for class categorization.

B. Few-shot classification problem formulation

Let D_{base} be a large dataset of labeled examples, commonly referred to as the source dataset, with the label space y_{base}. The classes in the source dataset are referred to as base classes. The objective of few-shot classification is to develop a model capable of leveraging the knowledge learned from D_{base} to learn from a very limited number of examples in a new class set. The training process typically consists of two stages: the training stage on D_{base} and the testing stage on an unseen target dataset, D_{test}, comprising a new set of classes, denoted as y_{test}, where $y_{base} \cap y_{test} = \emptyset$. In the testing stage, we employ episodic sampling, where a series of tasks is constructed from D_{test}. For each task, we construct a support set $S = \{(x_i, y_i)\}_{i=1}^{|NK|}$ by randomly sampling N classes from y_{test}. For each sampled class, K samples are randomly selected, resulting in an N-way K-shot classification task. Each task is accompanied by a query set, denoted as Q, sampled from the same classes for evaluation purposes.

C. Category-aware feature map reconstruction network

In the N-way K-shot image classification task, the support set consists of N classes, with each class containing K support images. Our objective is to predict the class label of a query image based on the N*K support images. We employ a convolutional feature extractor to extract the support feature maps, denoted as $F_{i,j}^S$, for the instances in the support set, as well as the query feature map, denoted as F^Q, for the query instance. Here, $F_{i,j}^S$ represents the feature map for the j-th instance of the i-th class in the support set. Each feature map $F \in R^{r \times d}$, where r denotes the spatial resolution of the feature map, and d represents the number of channels. Furthermore, we compute the prototype F_i^P for each class as the representative feature map of all instances belonging to that class.

$$F_i^P = \frac{1}{K} \sum_{j=1}^{K} F_{i,j}^S \tag{1}$$

Authorized licensed use limited to: JILIN UNIVERSITY. Downloaded on April 02,2024 at 06:48:38 UTC from IEEE Xplore. Restrictions apply.

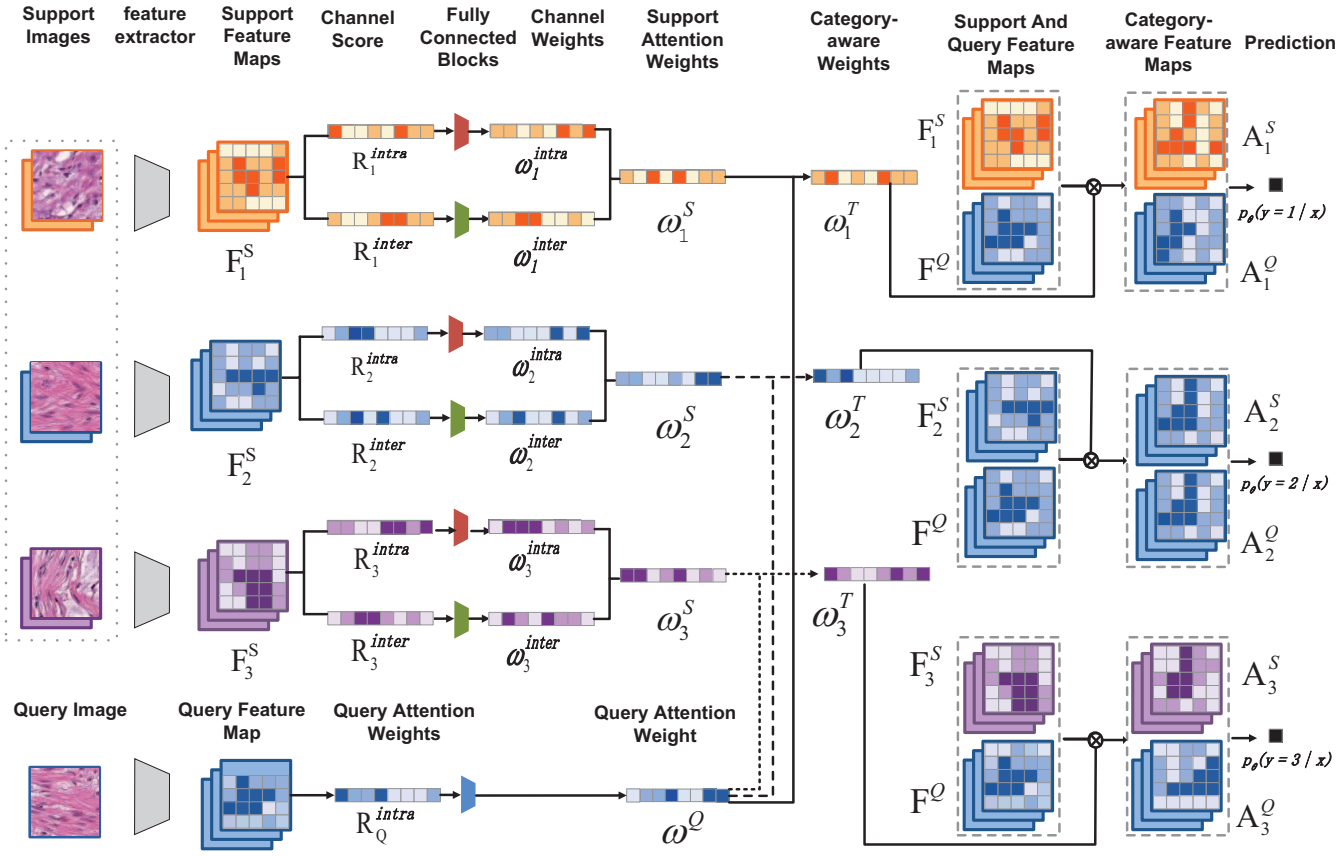


Fig. 1. Architecture overview of our proposed Category-Aware Feature Map Reconstruction Network.

where the prototype for c-th channel of the i-th class is denoted as $f_{i,c}^P \in R^r$. The mean spatial feature M_i^P to represent salient object regions is calculated as follows:

$$M_i^P = \frac{1}{C}\sum_{j=1}^{C} f_{i,j}^P \tag{2}$$

We can then calculate the intra-class channel score and the inter-class channel score. The intra-class channel score $R_{i,c}^{intra}$ for the c-th channel of the i-th class indicates the matching extent between highly activated regions on the channel and the salient region of the mean spatial feature. It is calculated as follows:

$$R_{i,c}^{intra} = \frac{1}{r}\|f_{i,c}^P - M_i^P\|^2 \tag{3}$$

The inter-class channel score $R_{i,c}^{inter}$ for the c-th channel of the i-th class indicates the extent to which the c-th channel contains distinct information for each class. It is calculated as follows:

$$R_{i,c}^{inter} = \frac{1}{r}\min_{1\le j\le N, j\neq i}\|f_{i,c}^P - M_j^P\|^2 \tag{4}$$

Intuitively, channels with higher discriminative power should possess lower intra-class variation scores and higher inter-class variation scores. We utilize these two scores to define the channel weights. The intra-class channel weights ω_i^{intra} and inter-class channel weights ω_i^{inter} are transformed by the corresponding channel scores and fully connected blocks b, as calculated below:

$$\omega_i^{intra} = b^{intra}\left(R_i^{intra}\right) \tag{5}$$

$$\omega_i^{inter} = b^{inter}\left(R_i^{inter}\right) \tag{6}$$

Finally, we can calculate the category-aware weight. category-aware weight ω_i^T of the i-th class is defined by a linear combination of the intra-class channel weight ω_i^{intra} and the inter-class channel weight ω_i^{inter}, with a balancing hyperparameter α as follows:

$$\omega_i^T = \alpha\omega_i^{intra} + (1-\alpha)\,\omega_i^{inter}, \alpha \in [0,1] \tag{7}$$

The feature map on the j-th image from class i of the support set is transformed by the category-aware weight ω_i^T for class i to generate the category-aware feature map $A_{i,j}^S$. This is calculated as follows:

$$A_{i,j}^S = \omega_i^T \odot F_{i,j}^S \tag{8}$$

Since the query set images are not labeled, to test whether the query image is the query image of the i-th class, we

Authorized licensed use limited to: JILIN UNIVERSITY. Downloaded on April 02,2024 at 06:48:38 UTC from IEEE Xplore. Restrictions apply.

combine the category-aware weights of the i-th class and the query feature map to generate the category-aware feature map A_i^Q, calculated as follows:

$$A_i^Q = \omega_i^T \odot F^Q \tag{9}$$

From the distance d between the category-aware feature maps $A_{i,j}^S$ and A_i^Q, we can calculate the probability that the query image belongs to class i as follows:

$$p_\theta\left(y = i \middle| x\right) = \frac{exp\left(-d\left(A_i^S, A_i^Q\right)\right)}{\sum_{j=1}^{N} exp\left(-d\left(A_j^S, A_j^Q\right)\right)} \tag{10}$$

III. Experiment

A. Materials and Implementation Details

To validate the performance of our proposed method in few-shot fine-grained histological image classification tasks, we constructed a histological few-shot dataset by selecting image samples from six histological datasets, namely CRC-TP [12], LC25000 [13], BreakHis [14], NCT-CRC [15], TCGA [16], and MLC [17]. This dataset encompasses diverse tissue types and organs, comprising a total of 34 cancer tissue categories. We randomly selected 14,686 images from these datasets for training, validation, and evaluation purposes. Please refer to Table 1 for detailed statistics. Considering future clinical applications, we deliberately chose test categories that are more similar in terms of image characteristics, instead of randomly selecting categories in the few-shot experiments. Specifically, 24 categories were used for training. Five categories were reserved for validation. Additionally, another five categories were used for testing.

TABLE I
COMPARISON WITH STATE-OF-THE-ART METHODS WITH 95% CONFIDENCE INTERVALS ON FIVE-WAY CLASSIFICATION FOR FEW-SHOT HISTOLOGICAL IMAGES DATASETS

Data set	Tissue classes number	Cancer types	Dataset
Training set	8	Breast	BreakHis
	2	stomach	TCGA
	7	Colon	CRC-TP
	4	Colon	NCT[32]
	3	lymph nodes	MLC
Validation set	5	Lung and Colon	LC2500[8]
Evaluation set	5	Colon	NCT[32]

For the n-way k-shot setting, each episode consists of n categories, with k support images per category. The training was conducted on a 5-way 10-shot configuration, with 16 query images. The hyperparameterα was set to 0.5. The images varied in size, ranging from 150x150 to 768x768, with various aspect ratios. For ease of model training, all images were preprocessed to a size of 84x84. Data augmentation techniques, including random cropping, horizontal flipping, and color jittering, were employed[18][19][20][21]. We randomly sampled 10,000 classification scenarios for few-shot classification and reported the average classification accuracy with a 95% confidence interval.

We implemented all experiments using PyTorch on an NVIDIA 3090 GPU. For image feature extraction, we employed Conv4 and ResNet12 as our backbone networks. Both backbone networks accept images of size 84x84; however, due to structural differences, they generate feature maps of different sizes. Conv4 consists of four convolutional blocks, each containing a convolutional layer with 64 channels, followed by batch normalization, ReLU activation, and max pooling, resulting in feature maps of size 64x5x5. On the other hand, ResNet12 comprises four residual blocks, each composed of three convolutional layers, producing feature maps of size 640x5x5. To compute channel weights, we utilized a fully connected block, including an input layer of size BxC, a fully connected layer of size Bx2C, a batch normalization layer of size Bx2C, a ReLU activation layer of size Bx2C, another fully connected layer of size BxC, and a Tanh activation layer of size BxC.

B. Quantitative and Qualitative Analysis

Table 2 presents the results of our proposed few-shot classification approach and other existing methods on the histological image few-shot dataset. In this experiment, we employed the optimization-based MAML method, the global feature-based ProtoNet method, the attention-based ResNet method, the local feature-based DeepEMD method, and the baseline FRN method, obtaining their results through publicly available code. We evaluated the classification accuracy of 5-way 1-shot, 5-way 5-shot, and 5-way 10-shot using Conv4 and ResNet12 as the feature extractors. Irrespective of the feature extractor employed, our method achieved the best performance across 1-shot, 5-shot, and 10-shot experiments. Notably, our approach achieved the highest accuracy of 90.23% in the 5-way 10-shot experiment when using ResNet12 as the feature extractor. Compared to the baseline FRN method, our method demonstrated performance improvements of 3.86%, 4.72%, and 3.86% in the 1-shot, 5-shot, and 10-shot scenarios, respectively, when Conv4 served as the backbone network. The performance gains were even more significant with ResNet12, resulting in a 9.36% improvement in the 1-shot experiment. The representative optimization-based MAML method for few-shot learning did not perform as well as the metric-based models in the histological image fine-grained classification task. Unlike other methods, the ProtoNet model exhibited diminished performance when ResNet12 was used as the feature extractor. The ReNet model showcased remarkable effectiveness in this experiment, owing to its two relational modules designed to capture discriminative regions in histological images, thereby demonstrating superior performance in fine-grained classification tasks.

Figure 2 presents the performance of ProtoNet, FRN, and our proposed method in the histological image few-shot classification task, considering different feature extractors (Conv4 and ResNet12) and varying numbers of support ways within the training set. The results demonstrate that as the number of support ways increases, only ProtoNet exhibits a gradual improvement in performance, whereas our proposed method

Authorized licensed use limited to: JILIN UNIVERSITY. Downloaded on April 02,2024 at 06:48:38 UTC from IEEE Xplore. Restrictions apply.

TABLE II
DETAILS OF FEW-SHOT HISTOLOGICAL IMAGE DATASET

Method	Venue	Backbone	5-way 1-shot	5-way 5-shot	5-way 10-shot
MAML	ICML'17	Conv4	52.34±1.23	59.13±0.84	63.41±0.77
		Resnet12	65.22±0.65	67.69±0.93	68.50±0.63
ProtoNet	NeurIPS'17	Conv4	55.68±0.43	76.66±0.65	80.2±0.21
		Resnet12	56.85±0.68	72.96±0.73	76.86±0.89
DeepEMD	CVPR'20	Resnet12	66.44±0.26	78.10±0.57	81.34±0.69
ReNet	ICCV'21	Resnet12	68.27±0.39	85.58±0.20	89.07±0.16
FRN	CVPR'21	Conv4	65.34±1.1	80.82±0.42	84.69±0.22
		Resnet12	64.19±0.87	81.89±0.12	84.99±0.43
Ours	Ours	Conv4	69.20±0.71	85.54±0.29	88.55±0.33
		Resnet12	73.55±0.94	87.99±0.11	90.23±0.15

and FRN achieve the best performance at 5-way, with a subsequent decline as the number of support ways increases. This observation can be attributed to ProtoNet's adoption of a global feature-based metric, which benefits from increased class information during each training iteration, facilitating the construction of prototypes. In contrast, the performance degradation of our proposed method and FRN with an increasing number of training set categories may indicate overfitting. Notably, when employing the more complex ResNet12 feature extractor, the performance decline associated with an increased number of training set categories is relatively mild compared to the use of the Conv4 feature extractor.

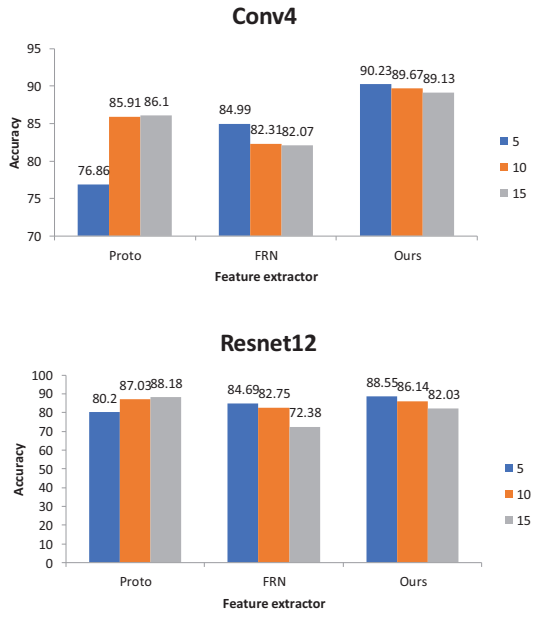


Fig. 2. Effect of the feature extractor and the number of support way in train set

1) Data agumentation: In the ablation study, we utilized ResNet12 as the feature extractor. Table 3 presents the impact of category-aware weights, intra-class channel weights, and inter-class channel weights on the experiments. The results indicate that the introduction of intra-class channel weights and inter-class channel weights both improved the classification accuracy. Specifically, in the 5-way 1-shot experiment, the intra-class channel weights and inter-class channel weights increased the accuracy of the baseline model by 5.91% and 6.75%, respectively. This finding demonstrates the helpfulness of identifying discriminative intra-class and inter-class channels for fine-grained classification tasks. Furthermore, the combination of intra-class channel weights and inter-class channel weights, forming the category-aware weights, achieved the highest improvement of 9.36% over the baseline model. This suggests that the intra-class and inter-class channel weights complement each other, and their combined effect plays a crucial role in accomplishing the few-shot fine-grained recognition task. This conclusion is also supported by Figure 3, which explores the influence of the balancing hyperparameter α on model performance. The category-aware weights are obtained by linearly combining the intra-class channel weights and inter-class channel weights with the balancing hyperparameter α. From Figure 3, we observe that the curve exhibits a convex shape, reaching its peak when α is 0.5, indicating the optimal classification performance. This implies that the contributions of intra-class channel weights and inter-class channel weights to category-aware weight are approximately equal.

TABLE III
EFFECT OF THE INTRA-CLASS CHANNEL WEIGHT,INTER-CLASS CHANNEL WEIGHT AND CATEGORY-AWARE WEIGHT

Intra-class channel weight	Inter-class channel weight	1-shot	5-shot	10-shot
—	—	64.19	81.89	84.99
✓	—	70.10	85.34	88.87
—	✓	70.94	86.12	89.73
✓	✓	**73.55**	**87.99**	**90.23**

Authorized licensed use limited to: JILIN UNIVERSITY. Downloaded on April 02,2024 at 06:48:38 UTC from IEEE Xplore. Restrictions apply.

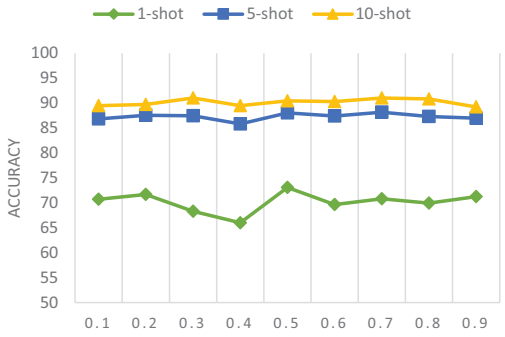


Fig. 3. Effect of balancing hyperparameters α

IV. Conclusion

In this study, we proposed a Category-Aware Feature Map Reconstruction Network method that leverages category-aware weights to localize inter-class differences in histological images. These weights are utilized for transforming the feature maps of support and query images. Finally, the classification prediction for query images is achieved by calculating the distance between the transformed support feature map and query feature map. Experimental results demonstrate the outstanding performance of our method on histological image few-shot datasets, with a test accuracy of 90.23% (when the test classes differ from the training classes), surpassing the baseline method by 5.24%. This method contributes to more accurate cancer diagnosis while reducing reliance on pathologists.

ACKNOWLEDGMENT

This work was supported by the National Key R&D Program of China under Grant Nos. 2021ZD0112501 and 2021ZD0112502; the National Natural Science Foundation of China under Grant Nos. U22A2098, 62172185 and 61876069; Jilin Province Capital Construction Fund Industry Technology Research and Development Project No. 2022C047-1; Changchun Key Scientific and Technological Research and Development Project under Grant No. 21ZGN30; and Jilin Province Natural Science Foundation under Grant No. 20200201036JC.

References

[1] Hanahan,D.: Hallmarks of Cancer: New Dimensions. Cancer Discovery 12(1),31-46(2022).
[2] Ferlay, J., Colombet, M., Soerjomataram, I., Parkin, D. M., Piñeros, M., Znaor, A., Bray, F et al:Cancer statistics for the year 2020: An overview. International journal of cancer 149(4),778-789(2021).
[3] Srinidhi, C. L., Ciga, O., Martel, A. L.: Deep neural network models for compu-tational histopathology: A survey. Medical Image Analysis 67,101813(2021).
[4] Finn, C., Abbeel, P., Levine, S.: Model-agnostic meta-learning for fast adapta-tion of deep networks. In: International conference on machine learning, pp.1126-1135.PMLR(2017).
[5] Snell, J., Swersky, K., Zemel, R.: Prototypical networks for few-shot learning. Advances in neural information processing systems 30(2017).
[6] Kang, D., Kwon, H., Min, J., Cho, M.: Relational embedding for few-shot clas-sification. In: Proceedings of the IEEE/CVF International Conference on Com-puter Vision,pp.8822-8833(2021).
[7] Zhang, C., Cai, Y., Lin, G., Shen, C.: DeepEMD: Few-shot image classification with differentiable Earth mover's distance and structured classifiers. In: Proceed-ings of the IEEE/CVF conference on computer vision and pattern recogni-tion,pp.12203-12213(2020).
[8] Wertheimer, D., Tang, L.,Hariharan, B.: Few-shot classification with feature map reconstruction networks. In: Proceedings of the IEEE/CVF Conference on Com-puter Vision and Pattern Recognition,pp.8012-8021(2021).
[9] Chao, S., Belanger, D.: Generalizing Few-Shot Classification of Whole-Genome Doubling Across Cancer Types. In: Proceedings of the IEEE/CVF International Conference on Computer Vision,pp.3382-3392(2021).
[10] Li, W., Wang, L., Xu, J., Huo, J., Gao, Y., Luo, J.: Revisiting local descriptor based image-to-class measure for few-shot learning. In: Proceedings of the IEEE/CVF Conference on Computer Vision and Pattern Recognition,pp.7260-7268(2019).
[11] Lee, S., Moon, W., Heo, J. P.: Task Discrepancy Maximization for Fine-grained Few-Shot Classification. In: Proceedings of the IEEE/CVF Conference on Com-puter Vision and Pattern Recognition,pp.5331-5340(2022).
[12] Javed, S., Mahmood, A., Werghi, N., Benes, K., Rajpoot, N.: Multiplex cel- lu-lar communities in multi-gigapixel colorectal cancer histology images for tissue phenotyping. IEEE Transactions on Image Processing 29,9204-9219(2020).
[13] Borkowski, A. A., Bui, M. M., Thomas, L. B., Wilson, C. P., DeLand, L. A., Mastorides, S. M.: Lung and Colon Cancer Histopathological Image Da-taset(LC25000).CoRR 1912.12142(2019).
[14] Spanhol, F. A., Oliveira, L. S., Petitjean, C., Heutte, L.: A dataset for breast cancer histopathological image classification. Ieee transactions on biomedical en-gineering 63(7),1455-1462(2015).
[15] Kather, J. N., Halama, N., Marx, A .: 100,000 histological images of human colorectal cancer and healthy tissue. Zenodo10 5281(2018).
[16] Kather, J. N., Pearson, A. T., Halama, N., Jäger, D., Krause, J., Loosen, S. H., et al: Deep learning can predict microsatellite instability directly from histology in gastrointestinal cancer. Nature medicine 25(7),1054-1056(2019).
[17] Orlov, N. V., Chen, W. W., Eckley, D. M., Macura, T. J., Shamir, L., Jaffe, E. S., Goldberg, I. G .: Automatic Classification of Lymphoma Images With Trans-form-Based Global Features. IEEE Transactions on Information Technology in Biomedicine 14(4),1003-1013(2010).
[18] Chen, W. Y., Liu, Y. C., Kira, Z., Wang, Y. C. F., & Huang, J. B.: A closer look at few-shot classification. arXiv preprint arXiv:1904.04232(2019).
[19] Wang, Y., Chao, W. L., Weinberger, K. Q., van der Maaten, L.: SimpleShot: Revisiting Nearest-Neighbor Classification for Few-Shot Learning. arXiv preprint arXiv:1911.04623(2019).
[20] Ye, H. J., Hu, H., Zhan, D. C., Sha, F.: Few-shot learning via embedding adap-tation with set-to-set functions. In: Proceedings of the IEEE/CVF conference on computer vision and pattern recognition,pp.8808-8817(2020).
[21] Zhang, C., Cai, Y., Lin, G., Shen, C.: Few-shot image classification with differ-entiable earth mover's distance and structured classifiers. In: Proceedings of the IEEE/CVF conference on computer vision and pattern recognition,pp.12203-12213(2020).

Authorized licensed use limited to: JILIN UNIVERSITY. Downloaded on April 02,2024 at 06:48:38 UTC from IEEE Xplore. Restrictions apply.